

ADAPTIVE SPACE-TIME ELEMENTS IN THE DYNAMIC ELASTIC-VISCOPLASTIC PROBLEM

C. BAJER,† R. BOGACZ† and C. BONTHOUX‡

†Institute of Fundamental Technological Research, Polish Academy of Sciences, Świętokrzyska 21, PL-00-049 Warsaw, Poland

‡Ecole Nationale Supérieure d'Electricité et de Mécanique, B.P. 850, 54011 Nancy Cedex, France

(Received 22 February 1990)

Abstract—An adaptive technique for the solution of the dynamic elastic-viscoplastic problem has been developed. The mesh modification is performed by the use of the space-time element method according to error estimation. The number of joints is preserved and the mesh is refined in regions of high stress gradients. This enables the size of the problem to be reduced and increases the speed of computations. The incremental procedure in the case of a small time step allows the nonlinear path iteration to be associated with the time marching scheme. The remesh and remap problems related to stresses are described. Numerical examples of a plane strain rolling contact problem and collision of the plane strain object prove the efficiency of the approach.

1. INTRODUCTION

If one wants to treat a phenomenon in a numerical manner with a required accuracy several computations problems must be solved. The fundamental one is the mesh condensation required particularly in the zone of great stress gradients to investigate processes occurring. The traveling load, shocks, and contact problems are characteristic of fast varying stress fields over the domain. Mesh condensation is, among others, a convenient method by which to achieve the increase of the accuracy. However, a technique with a fixed fine mesh is time consuming, especially if applied to nonlinear problems. Large plastic deformations and flow of the material occurring in some regions can destroy the mesh if it is assigned to the material points. From these reasons moving mesh methods were developed (see for example [1, 2]). In this approach the condensed grid moves with the feature of interest, leaving the coarse mesh in the remainder of the structure.

The group of problems in which moving mesh methods could be successfully applied are contact phenomena in the case of a traveling contact zone. Since contact forces or reactions of considerable value are applied to nodal points it is necessary to reduce the distances between the joints that are in contact over the entire path of the load, which strongly increases the computational effort involved. It should be emphasized that contact problems require a sufficiently small step of the time integration of the motion equation.

Adaptive generation of the mesh is assumed for the described approach. The approximation error is estimated in each time step and, depending on its value, the mesh is modified. So called r -adaptation

preserves the number of joints and moves the nodal points towards the domains of higher stress gradients.

Adaptive techniques are known and commonly applied mainly to parabolic and elliptic problems. In the presented approach the mesh adaptation is performed by the space-time element method (STEM) and is applied to structural dynamics. Simplex-shaped elements are applied. This allows one to obtain directly the system of separated algebraic equations that can be solved with the joint-by-joint scheme [3, 4]. The STEM enables mesh modification in each step in a natural way [5]. This means that joints of the spatial mesh taken at two successive times are connected and in this way the space-time subdomains can be determined. Since the joints have different coordinates at times that limit the time layer at the top and the bottom, the space-time elements have non-rectangular forms. However, the method is conditionally stable considering both the time step and the speed of mesh modification [6]. In the class of problems treated in the present paper neither of the limitations are reached.

The space-time element approach can be considered as a time-continuous Galerkin method. It differs from the time-discontinuous Galerkin method [7, 8] which leads to A -stable higher order accurate ordinary differential equation solvers but in turn gives uneconomically large matrices. Moreover, the generalization of the time-continuous Galerkin method to elastodynamics seems possible only in some circumstances.

2. SPACE-TIME ELEMENT APPROXIMATION

A typical time integration procedure applied to a nonlinear problem requires force balance in every

time step. Especially when the plastic flow is taken into account, the exact evaluation of the contact stress state is essential. When the time step is large the iterative procedure is necessary to evaluate the equilibrium state of the nonlinear process [9]. When the time step is small enough, the residual forces are also small and the whole iteration can be reduced to only one step, preserving the negligible error.

Since the method described below was originally developed for the contact problem in which the contact zone can vary and a small time step is forced by the contact phenomenon, the one-step procedure was assumed to determine the strain increments. However, although the full iteration can be applied, it increases the computational time considerably. In problems of large deformations the element matrices must be recalculated at each time step. This effort can be simultaneously spent for mesh adaptation.

The time marching procedure for nonlinear problems is described below. The elastic-viscoplastic material model assumed can be simply replaced by any other.

2.1. Incremental procedure

Let us consider the time layer $t_i \leq t \leq t_i + \Delta t = t_{i+1}$ (Fig. 1). The equation of virtual work can be written in the form

$$\int_{V_{t_i}} (\mathbf{S}_{t_i}(t) \delta \epsilon_{t_i} + \rho_{t_i} \ddot{\mathbf{u}}_{t_i}(t) \delta \mathbf{u}_{t_i}) dV_{t_i} = R(t) \quad (1)$$

$\mathbf{S}_{t_i}(t)$ = second Piola-Kirchhoff stress tensor in time t related to configuration t_i

$\epsilon_{t_i}(t)$ = Green-Lagrange strain tensor

ρ_{t_i} = mass density in time t_i

$R(t)$ = virtual work of the external forces

$$R(t) = \int_{V_i} f_i^B(t) \delta u_i dV_i + \int_{S_i} f_i^S(t) \delta u_i dS_i$$

$f_i^B(t)$ and $f_i^S(t)$ are components of the externally applied body and surface forces in time t . Equation (1) can be integrated over the time interval $[t_i, t_{i+1}]$. The incremental decomposition

$$\begin{aligned} \mathbf{S}_{t_i}(t) &= \mathbf{S}_{t_i}(t_i) + \Delta \mathbf{S} = \boldsymbol{\tau}_{t_i} + \Delta \mathbf{S} \\ \epsilon_{t_i}(t) &= \Delta \epsilon \\ \mathbf{u}_{t_i}(t) &= \mathbf{u}_{t_i}(t_i) + \Delta \mathbf{u} \end{aligned} \quad (2)$$

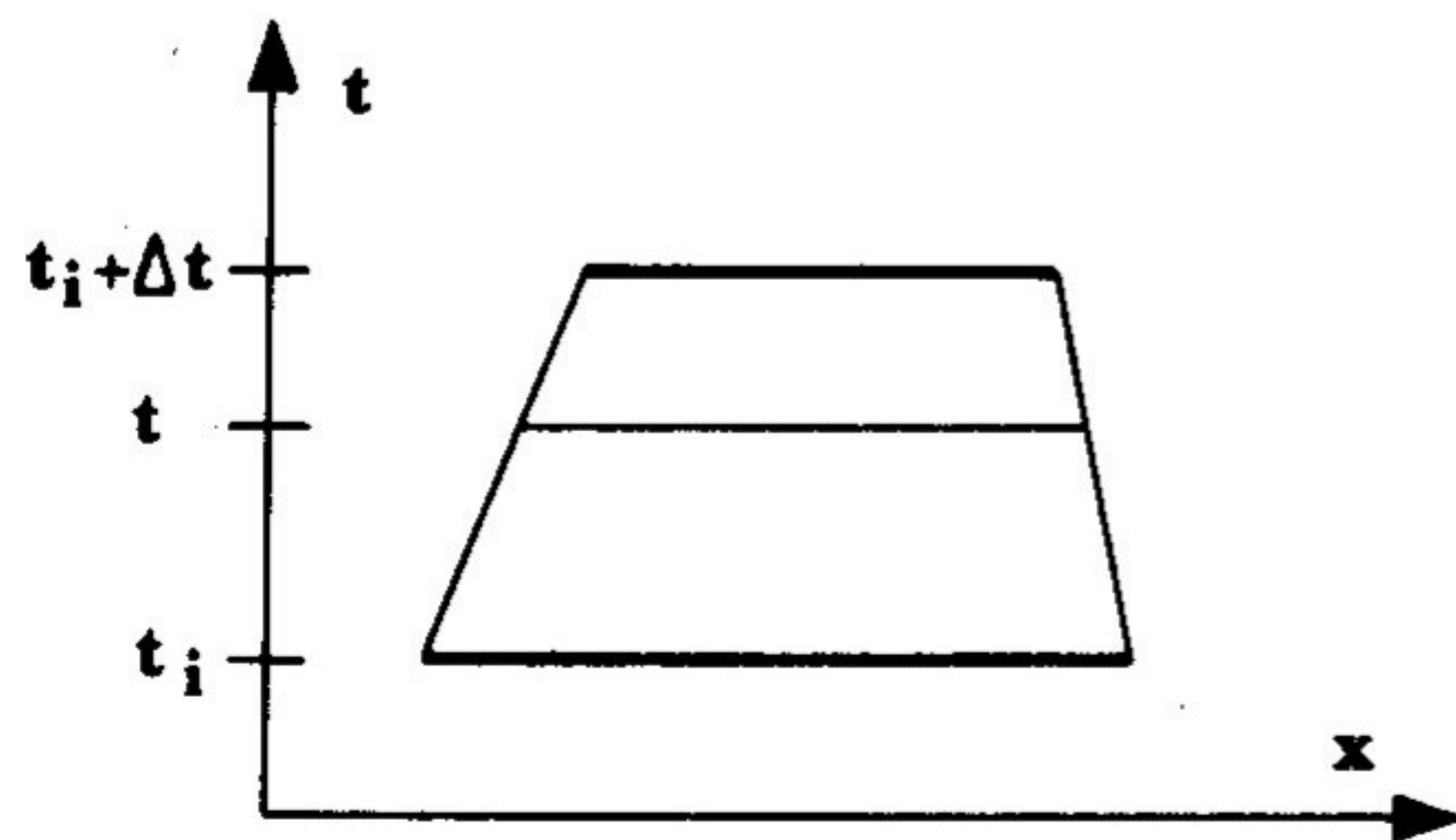


Fig. 1. Non-rectangular space-time element of uni-dimensional object.

and the constitutive relation

$$\Delta \mathbf{S} = \mathbf{C}_{t_i} \Delta \epsilon \quad (3)$$

are also assumed. Finally eqn (1) has the form

$$\begin{aligned} & \int_{t_i}^{t_i + \Delta t} \int_{V_{t_i}} \tau_{t_i} \delta(\Delta \epsilon) dV_{t_i} dt \\ & + \int_{t_i}^{t_i + \Delta t} \int_{V_{t_i}} \Delta \mathbf{S} \delta(\Delta \epsilon) dV_{t_i} dt \\ & + \int_{t_i}^{t_i + \Delta t} \int_{V_{t_i}} \rho_{t_i} \ddot{\mathbf{u}}_{t_i}(t) \delta(\Delta \mathbf{u}) dV_{t_i} dt \\ & + \int_{t_i}^{t_i + \Delta t} \int_{V_{t_i}} \rho_{t_i} \Delta \mathbf{u} \delta(\Delta \mathbf{u}) dV_{t_i} dt \\ & = \int_{t_i}^{t_i + \Delta t} R(t) dt. \end{aligned} \quad (4)$$

The double integral $\int_{t_i}^{t_i + \Delta t} \int_{V_{t_i}}$ can be replaced by the integral over the space-time domain $\Omega_i = \{\mathbf{x}, t: \mathbf{x} \in V_i, t_i \leq t \leq t_i + \Delta t\}$. The strain $\Delta \epsilon$ is split into a linear and nonlinear part

$$\Delta \epsilon = \Delta \mathbf{e} + \Delta \eta. \quad (5)$$

Applying eqns (3) and (5), neglecting higher order small terms and integrating by parts, we obtain

$$\begin{aligned} & \int_{\Omega_i} \tau_{t_i} \delta(\Delta \epsilon) d\Omega_i + \int_{\Omega_i} \mathbf{C}_{t_i} \Delta \mathbf{e} \delta(\Delta \mathbf{e}) d\Omega_i \\ & - \int_{\Omega_i} \rho_{t_i} \dot{\mathbf{u}}_{t_i}(t) \delta(\Delta \dot{\mathbf{u}}) d\Omega_i - \int_{\Omega_i} \rho_{t_i} \Delta \dot{\mathbf{u}} \delta(\Delta \dot{\mathbf{u}}) d\Omega_i \\ & = \mathbf{Q}_i - \int_{\Omega_i} \tau_{t_i} \delta(\Delta \eta) d\Omega_i. \end{aligned} \quad (6)$$

Let us denote the nodal displacements in the space-time element by \mathbf{q}_i . The vector \mathbf{q}_i couples displacement increments at times that bound the time layer i from the bottom and the top. The displacements in the interior are expressed by the interpolation

$$\mathbf{u} = \mathbf{N}(\mathbf{x}, t) \mathbf{q} = \mathbf{N}(\mathbf{x}, t) \begin{Bmatrix} \mathbf{q}^{\text{ante}} \\ \mathbf{q}^{\text{post}} \end{Bmatrix}. \quad (7)$$

This leads to the relations

$$\epsilon = D \mathbf{u} \quad \mathbf{S} = \mathbf{C} \epsilon \quad \mathbf{e} = D_N \mathbf{u}. \quad (8)$$

$D(x)$ and $D_N(x)$ are the linear and nonlinear differential operator, respectively. The force equilibrium

equation

$$\left[\int_{\Omega_i} (DN)^T C D N d\Omega_i + \int_{\Omega_i} (D_N N)^T \tau D_N N d\Omega_i - \int_{\Omega_i} \left(\frac{\partial N}{\partial t} \right)^T \rho \frac{\partial N}{\partial t} d\Omega_i \right] \Delta \mathbf{q} = \mathbf{F} - \int_{\Omega_i} (DN)^T \hat{\tau} d\Omega_i + \left[\int_{\Omega_i} \left(\frac{\partial N}{\partial t} \right)^T \rho \frac{\partial N}{\partial t} d\Omega_i \right] \mathbf{q} \quad (9)$$

can be written in a short form

$$(\mathbf{K}_L^i + \mathbf{K}_{NL}^i + \mathbf{M}^i) \Delta \mathbf{q}^i = \Delta \mathbf{F} - (\mathbf{F}_N^i + \mathbf{M}^i \mathbf{q}^i - \mathbf{F}^i), \quad (10)$$

where

$$\begin{aligned} \mathbf{K}_L^i &= \int_{\Omega_i} (DN)^T C D N d\Omega_i \\ \mathbf{K}_{NL}^i &= \int_{\Omega_i} (D_N N)^T \tau D_N N d\Omega_i \\ \mathbf{M}_i &= - \int_{\Omega_i} \left(\frac{\partial N}{\partial t} \right)^T \rho \frac{\partial N}{\partial t} d\Omega_i \\ \mathbf{F}_N &= \int_{\Omega_i} (DN)^T \hat{\tau} d\Omega_i. \end{aligned} \quad (11)$$

We must emphasize that the load vector \mathbf{F} in eqn (10) exactly represents impulse components, the dimension of which is Nsec. Hence the linear \mathbf{K}_L and nonlinear \mathbf{K}_{NL} stiffness matrices have a dimension of Nsec/m and the mass matrix \mathbf{M} is in kg/sec.

The step-by-step algorithm is described by the following formula:

$$\mathbf{C}_{i-1} \Delta \mathbf{q}_{i-1} + (\mathbf{D}_{i-1} + \mathbf{A}_i) \Delta \mathbf{q}_i + \mathbf{B}_i \Delta \mathbf{q}_{i+1} = \Delta \mathbf{F}_i + \mathbf{F}_i - \mathbf{F}_i^K - \mathbf{F}_i^M. \quad (12)$$

Index i denotes the number of the time step, $\Delta \mathbf{q}_i$ is the incremental displacement vector in time t_i . \mathbf{F}_i^K accumulates the internal forces and \mathbf{F}_i^M accumulates the increments of nodal forces contributed by inertia and damping. These vectors are described below

$$\begin{aligned} \mathbf{F}_i^K &= \sum_{n=1}^i [\mathbf{C}_{n-2}^K \Delta \mathbf{q}_{n-2} \\ &+ (\mathbf{D}_{n-2}^K + \mathbf{A}_{n-1}^K) \Delta \mathbf{q}_{n-1} + \mathbf{B}_{n-1}^K \Delta \mathbf{q}_n] \end{aligned} \quad (13)$$

$$\begin{aligned} \mathbf{F}_i^M &= \sum_{n=1}^i [\mathbf{C}_{n-2}^M \Delta \mathbf{q}_{n-2} \\ &+ (\mathbf{D}_{n-2}^M + \mathbf{A}_{n-1}^M) \Delta \mathbf{q}_{n-1} + \mathbf{B}_{n-1}^M \Delta \mathbf{q}_n]. \end{aligned} \quad (14)$$

Matrices \mathbf{A} , \mathbf{B} , \mathbf{C} and \mathbf{D} are the upper left, upper right, lower left and lower right submatrices, respectively, related to the *ante* and *post* moments [3]. Superscript K indicates the stiffness matrix

contribution and M indicates the inertia and damping contribution.

2.2. Viscoplasticity

The elastic-viscoplastic property of the material behaviour is assumed. The formulas primary described in [10, 11] and then applied for numerical purposes by Zienkiewicz (for example [12]) will be presented in brief below.

The velocity of viscoplastic strain can be written as

$$\dot{\epsilon}^{vp} = \gamma \left\langle \Phi \left(\frac{F}{\sigma_y} \right) \right\rangle \frac{\partial F}{\partial \sigma}. \quad (15)$$

γ is a linear creep coefficient ($\gamma = 10^{-5} - 10^{-3}$). The flow function for the plane strain $F = (3I_2)^{1/2} - \sigma_y$ (σ_y is a yield stress). The function Φ is assumed as an exponential one

$$\Phi \left(\frac{F}{\sigma_y} \right) = \left(\frac{F}{\sigma_y} \right)^N. \quad (16)$$

Depending on the flow function F the expression $\langle \cdot \rangle$ is equal to

$$\begin{aligned} F < 0: & \quad \langle \cdot \rangle = 0 \\ F \geq 0: & \quad \langle \cdot \rangle = \Phi \end{aligned} \quad (17)$$

The stress increment $\Delta \sigma$ which is accumulated can be solved by the relation

$$\Delta \sigma = \mathbf{E} D N \Delta \mathbf{u} - \mathbf{E} \Delta \epsilon^{vp} \Delta t. \quad (18)$$

3. MESH ADAPTATION

3.1. Error estimation

The formula engaged in the error estimation procedure should be rapid. Otherwise since it is applied in every computational step it would strongly increase computational times. If we denote by h the dimension of the mesh, the distribution of the error is given by the integral

$$\int_A h(u_{xx}^2 + u_{yy}^2) dx dy = \text{const}. \quad (19)$$

Applying the interpolation formulas to eqn (19) we obtain the value of the error in a joint.

$$e_i = \left[\sum_k \left(\sum_m \int_{A_m} \sum_j N_{,k}^i N_{,k}^j u_k^j dA_m \right)^2 \right]^{1/2}. \quad (20)$$

j denotes the number of the joint in the element m to which the joint i belongs. k is the x or y coordinate. The shape functions are linear, the derivatives $N_{,k}$ are constant and in such a case formula (20) can be given explicitly. This considerably increases the speed of calculations. In further applications we use eqn (20) as the error estimator.

Another approach is presented by Zienkiewicz *et al.* [13–15]. The error is estimated by the energy norm. The difference between the accurate and received stresses $\sigma - \hat{\sigma}$ is replaced by the estimate difference $\sigma^* - \hat{\sigma}$, where σ^* is a good approximation to the accurate solution. It can be obtained by a chosen averaging procedure. Thus the error distribution is related to finite elements. The given formulation can be applied alternatively.

3.2. Remeshing

The modification of the mesh is described in the following steps.

1. Evaluation of nodal errors.
2. Normalization of nodal error values.
3. Calculation of joint components of movement toward points of high errors. The nodal point that is considered is placed in the center of gravity of adjacent joints weighted with the nodal errors.
4. Verification of the mesh distortion. Dubious joints are relocated to construct the correct mesh in the neighborhood.

An additional requirement is that the contour must be preserved. The node lying on the boundary should remain there after remeshing. It is obvious that corners must be untouched. Two stage of operations allow the adapted and deformed mesh to be prevented from distortions and non-proportional element dimensions.

First we must select the nodes that are placed in regions where the faults in the mesh were detected, the relocation of which improves the mesh properties. A simple and efficient algorithm was published by Benson [16]. It detects the shear and volumetric distortion. Results are assigned to joints. Although the relations given by Benson are determined for a quadrangular mesh, they can be successfully applied for a triangular mesh taking into consideration its quadrilateral form based on couples of triangles.

Volumetric distortion R_v is determined as the quotient of the smallest area to the largest area of the quadrangle surrounding the node (Fig. 2).

$$R_v = \frac{\min(A_1, A_2, A_3, A_4)}{\max(A_1, A_2, A_3, A_4)} \quad (21)$$

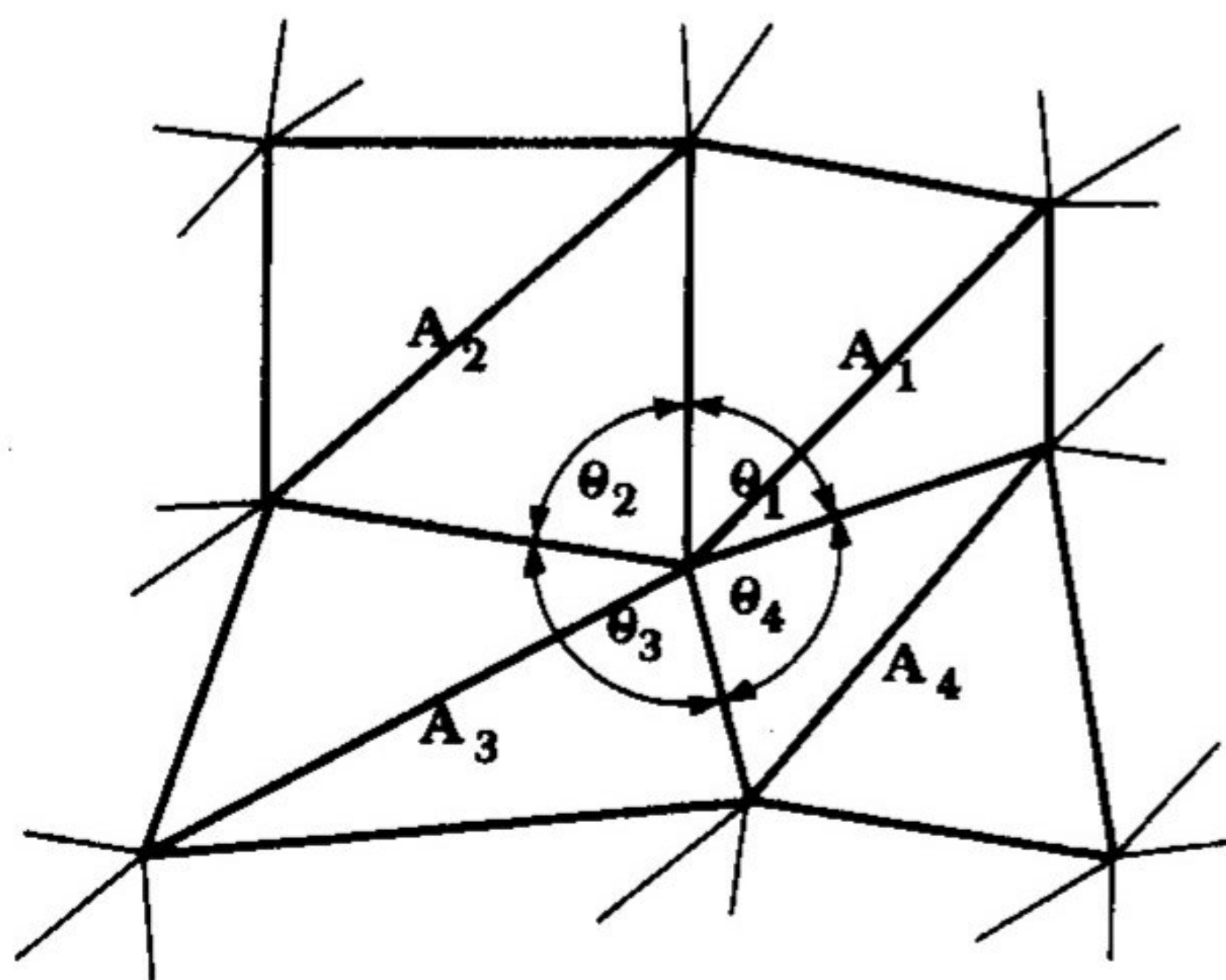


Fig. 2. Quadrilateral mesh tested for distortion.

$$\begin{aligned} A_1 &= \mathbf{v}_1 \times \mathbf{v}_2, & A_2 &= \mathbf{v}_2 \times \mathbf{v}_3, \\ A_3 &= \mathbf{v}_3 \times \mathbf{v}_4, & A_4 &= \mathbf{v}_4 \times \mathbf{v}_1. \end{aligned} \quad (22)$$

Shear distortion is determined by calculating the minimum sine of the angles formed by the corners of the elements surrounding the node

$$\begin{aligned} \sin \theta_1 &= \frac{A_1}{\|\mathbf{v}_1\| \|\mathbf{v}_2\|} \\ \sin \theta_2 &= \frac{A_2}{\|\mathbf{v}_2\| \|\mathbf{v}_3\|} \\ \sin \theta_3 &= \frac{A_3}{\|\mathbf{v}_3\| \|\mathbf{v}_4\|} \\ \sin \theta_4 &= \frac{A_4}{\|\mathbf{v}_4\| \|\mathbf{v}_1\|} \end{aligned} \quad (23)$$

$$R_\theta = \min(\sin \theta_1, \sin \theta_2, \sin \theta_3, \sin \theta_4). \quad (24)$$

Comparing the sine of angles we prevent the elements from having both acute and obtuse angles. This helps to avoid inverting the elements.

The following restrictions must be checked in every step to avoid mesh degeneration and loss of stability.

1. Maximum value of nodal movement d_{\max} in one step (c is the wave speed)

$$d_{\max} = c \Delta t / \beta_1. \quad (25)$$

2. Minimum element size b_{\min}

$$b_{\min} = \beta_2 c \Delta t. \quad (26)$$

3. Volumetric distortion

$$R_v^{\min} > R_v^0. \quad (27)$$

4. Shear distortion

$$R_\theta^{\min} > R_\theta^0. \quad (28)$$

The safety factors β_1, β_2 should be greater than 1; R_v^0 and R_θ^0 can be assumed as 0.5.

3.3. The remap problem

The generation of a mesh which is different from the mesh in the previous step that allows one to continue calculations with smaller approximation error is the first stage of calculations based on the mesh with modified geometry. The second stage, to be discussed below, is the projection of stress components to new domains.

There are several fundamental requirements that the remap algorithm should meet.

- The remap procedure must be efficient since it is applied in every step.
- Remapping must be accurate.

- The remap algorithm should be conservative. The integral of any quantity over the spatial domain should remain unchanged after remapping.
- The stability criteria limit the distance of the node movement in a time step.
- The algorithm should be consistent. This means that if the new mesh is identical to the original one then the projection cannot change the quantities.

In our case the stress vector is the only quantity to be remapped. If we had point forces, the remapping would be trivial. However, the stresses that cannot be concentrated in joints and after remeshing redistributed back over element areas complicate the problem.

We assume that the distance of joint movement is much smaller than the spatial size of the triangle. This allows one to compute the required values with the error of the lower range. The approximate formula was admitted to shorten the computational time

$$\sigma_i^+ = \frac{1}{A_i^+} \left[\sigma_i^- A_i^- + \sum_{j=1}^3 (\sigma_j^- - \sigma_i^-) \Delta A_j^- \right]. \quad (29)$$

ΔA_j^- denotes the area increment in the former mesh which is equal to zero when it covers the element domain in new geometry A_i^+ and is positive in another case (see Fig. 3). It is placed between two elements and is taken into account once. It can be noticed that near the corners the computations are not accurate. However, the influence of this simplification on the final results is negligible. We can see that when the subareas determined by the crossing edges of triangles are considered with accuracy (that may be troublesome) formula (29) is accurate, efficient, conservative and consistent.

4. NUMERICAL EFFICIENCY

The numerical efficiency is one of the fundamental features that must be taken into consideration in the solution of nonlinear problems. Calculation of one time step in every space-time finite element solution consists of two stages: formulation of global matrices after modification of the geometry as well as material properties and the solution of the system of algebraic

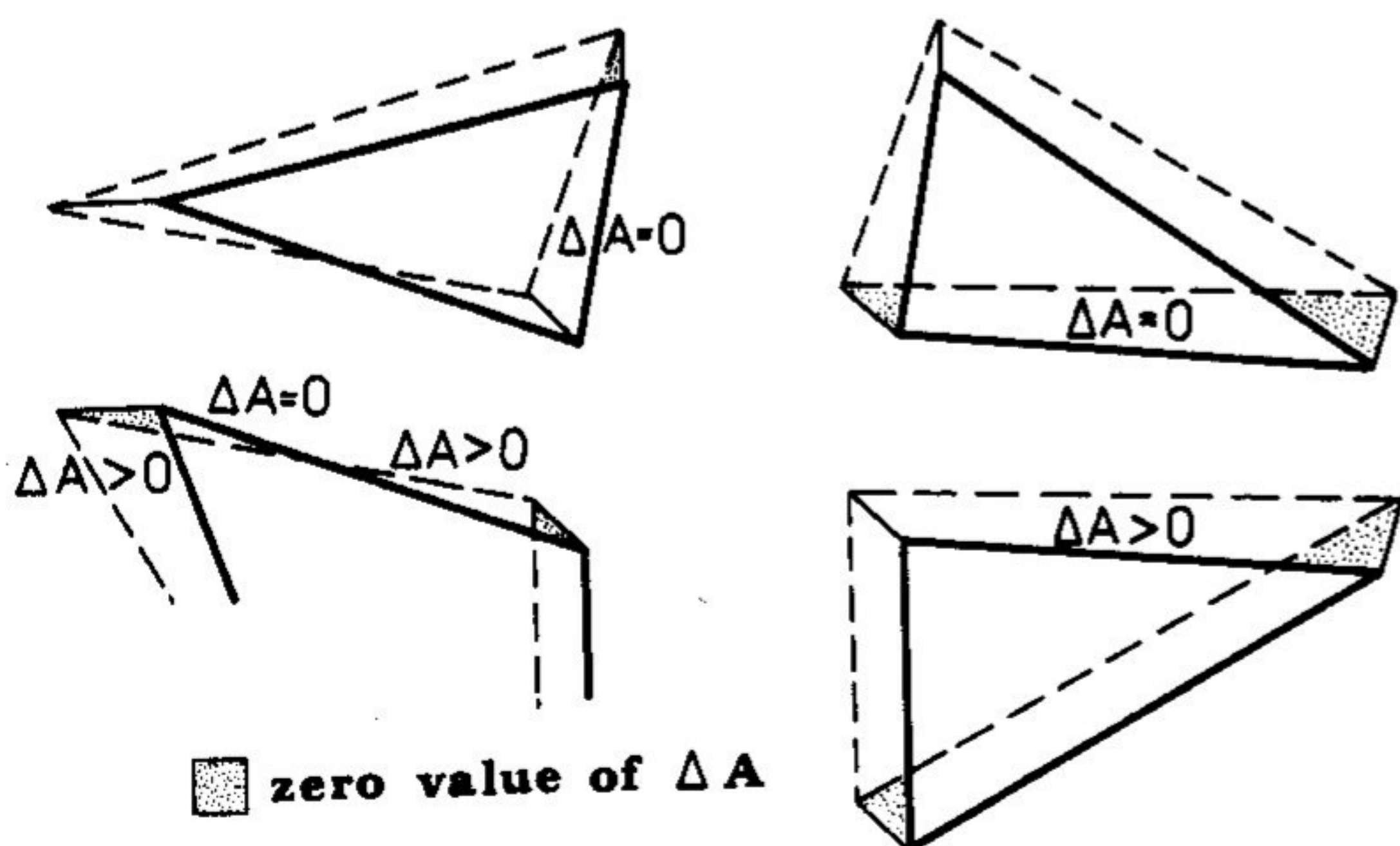


Fig. 3. Area increments in the remapping.

equations. Consideration of the form of the mass matrix and the method of damping is essential to the cost of the solution. The diagonal mass matrix and numerical damping enable fast calculation of the resulting displacement vector. The equations in the system can be decoupled if the explicit method of time integration is applied. However, in some problems the consistent mass matrix, and consequently described damping, is required. In such a case the full solution of the system of equations increases the computational cost.

Looking at the algorithm we can estimate the number of arithmetical operations per computational step. The number of multiplications M for the solution of displacements only (without evaluation of coefficients) depends on the required storage capacity. It is

$$M = 2sN(c + 1), \quad (30)$$

while $3.5sN(c + 1) + 1.5sN$ numbers are held and

$$M = 3sN(c + 1), \quad (31)$$

while $1.5sN(c + 1)$ numbers are held. c is the number of adjacent joints in the mesh; N is the total number of degrees of freedom and s is the nodal number of degrees of freedom.

The cost comparison of the space-time solution with the general numerical method of time integration is discussed below. The following assumptions define the general time integration method:

1. The element and global matrices exhibit symmetry.
2. The regular band of the global matrix is held.
3. The consistent mass matrix that forces, among others, the solution of the system of equations.
4. Damping is not considered.
5. There is optimum joint numbering for the minimum band width.
6. Multiplications by zero in the band are not eliminated.
7. The central difference scheme was assumed as a solution procedure.

The cost relation is depicted in Fig. 4. The slope of the cost of STEM is smaller than the cost slope for the central difference method. For a greater number of joints the crossing point of the two curves exhibits the higher efficiency of the STEM. The Gauss procedure engaged in the CDM gives the greatest cost contribution. In the case of other time integration procedures the comparison can be less optimistic. However, it must be emphasized that the cost of the solution by the STEM is linearly dependent on the number of joints (with no respect to the dimensionality of the structure).

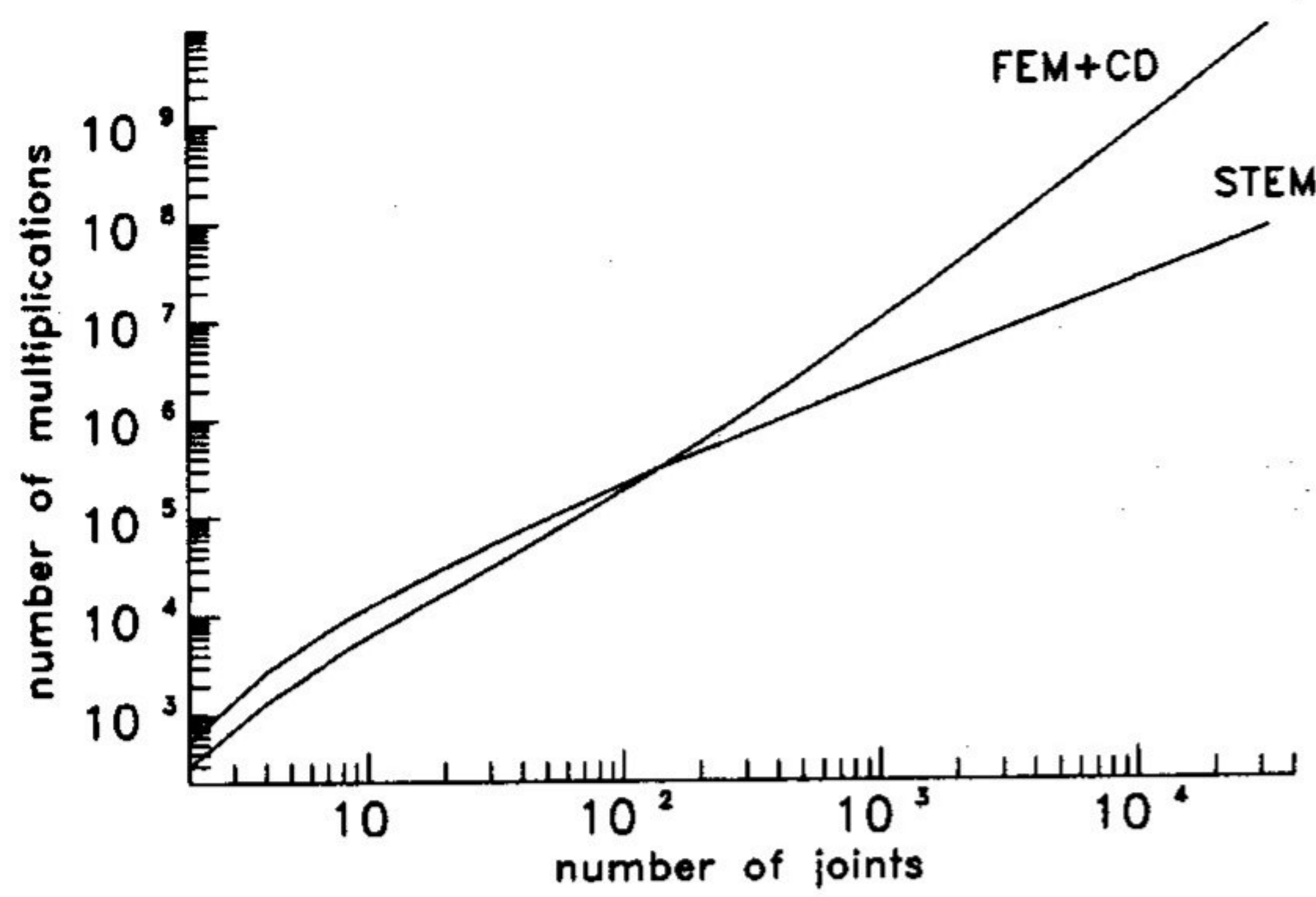


Fig. 4. The cost of the space-time element method: the finite element method + central difference method (FEM + CD) and the space-time element method (STEM).

5. NUMERICAL EXAMPLES

Several numerical examples prove the efficiency of the applied approach. At first simple testing problems were solved to exhibit the phenomena accompanying the numerical algorithm. This is more important especially when we cannot distinguish the numerical instability effects from the physical ones. The influence of damping coefficients can be simply shown when non-complicated structures are solved.

Examples of real engineering problems are presented below. Material non-linearities and unilateral contact are considered together with the adaptive mesh modification technique.

5.1. Elastic-viscoplastic rolling

In this example rolling of the plane strain strip by the rigid roller was considered (Fig. 5). The contact condition was realized by the force penalty function. The Coulomb friction was assumed in the contact zone. The following numerical data were assumed in the example: $E = 2.05$, $\nu = 0.3$, $\rho = 7.83$, $\eta_z = 0.2$ (external damping coefficient), $\gamma = 5 \times 10^{-4}$, $\mu = 0.5$ (Coulomb friction factor), $N = 1$, $\sigma_y = 0.0042$. Results are depicted in Figs 6-8.

5.2. Bar collision

We consider a symmetric rectangular plane strain object made of elastic-viscoplastic material (Fig. 9) moving with a speed v toward the rigid wall. First computations were performed to show the influence of the mesh and the time step on the results. The horizontal displacement of the end point placed on

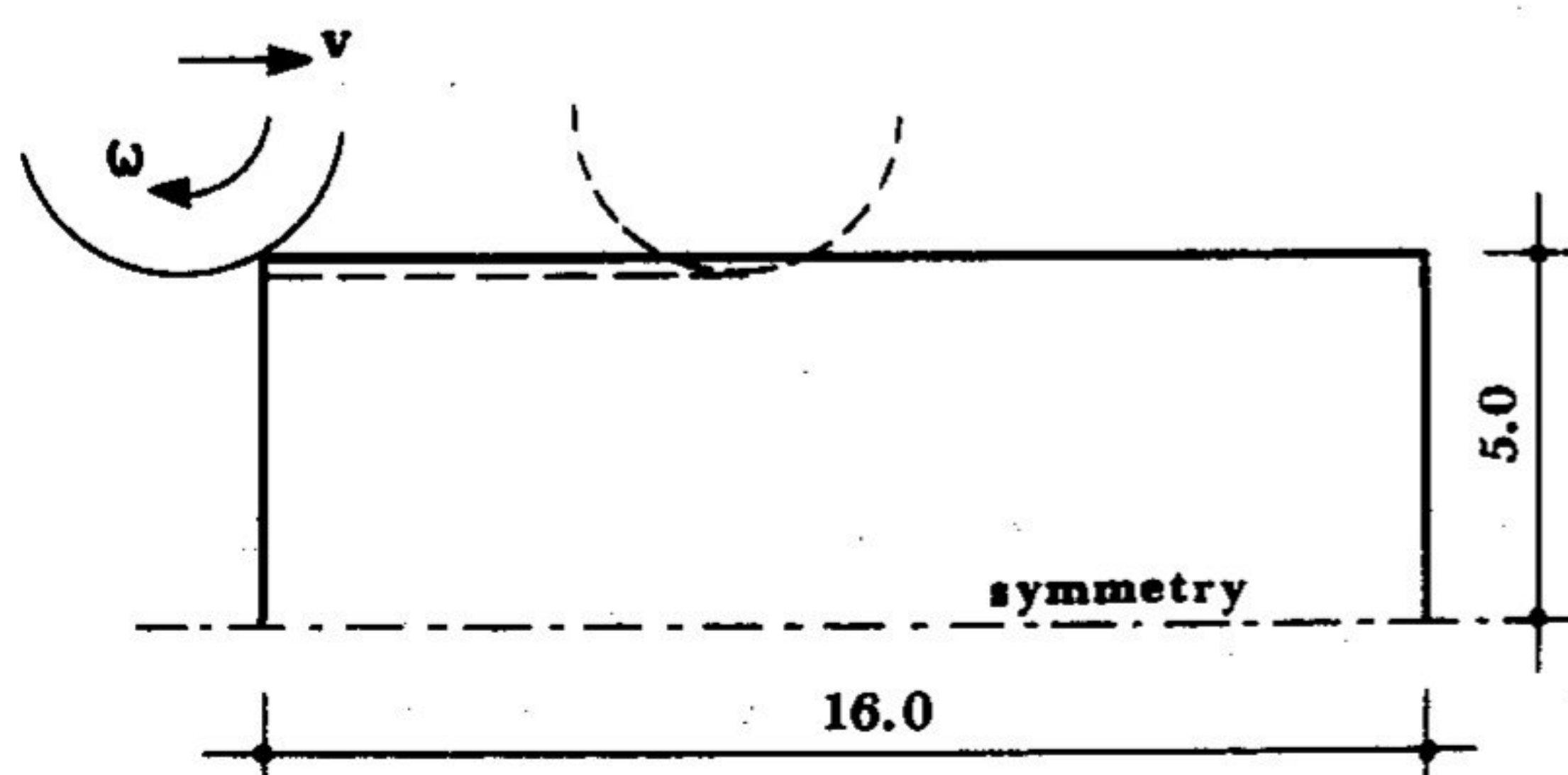


Fig. 5. The plane strip in the rolling process.

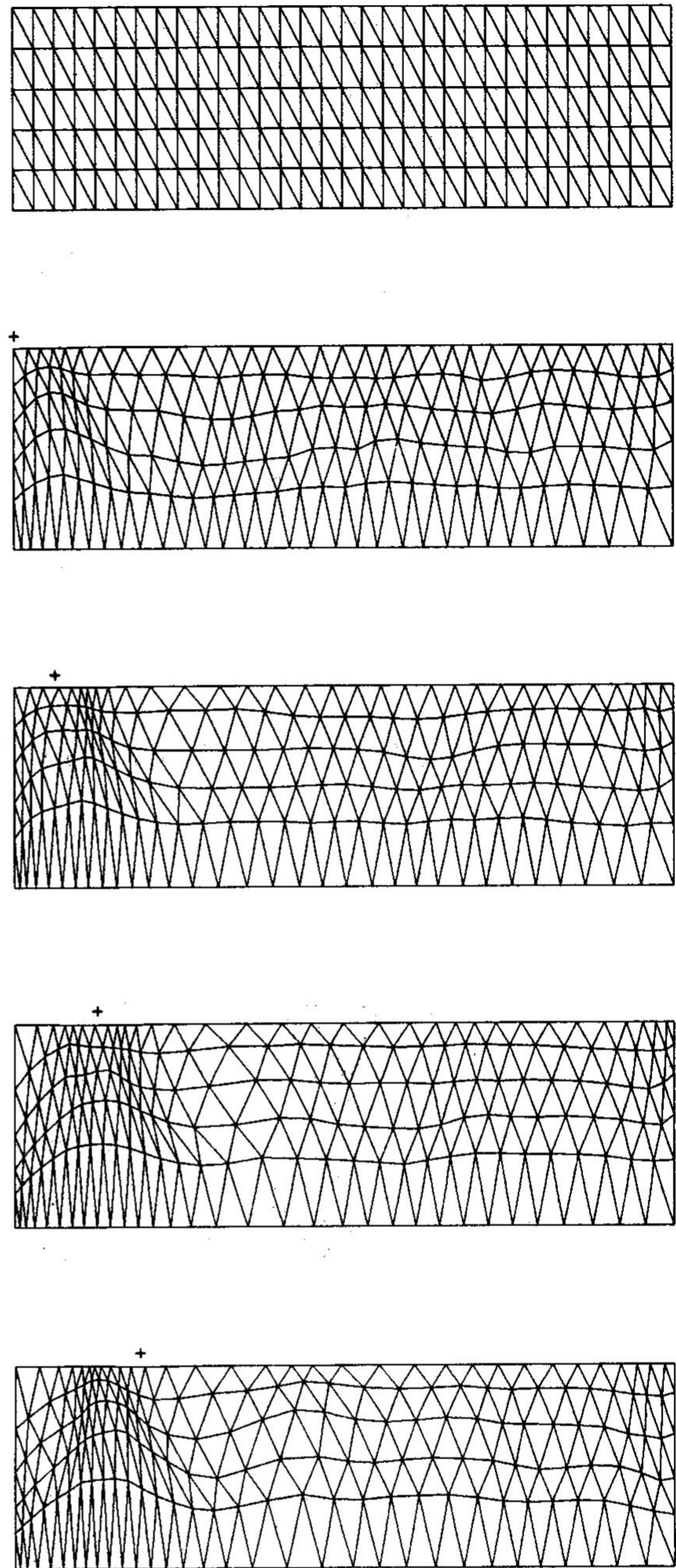


Fig. 6. The mesh before and after remeshing ('+' denotes the position of the centre of the roller).

the symmetry axis was investigated. Figure 10 exhibits the influence of the γ factor on the solution. Figure 11 shows the influence of the time step when γ is equal to 5×10^{-3} . Results for successively condensed mesh (4×1 , 8×2 and 16×4 squares divided into triangles) with $\gamma = 5 \times 10^{-4}$ and $\Delta t = 0.1$ are depicted in Fig. 12. In all these tests the constant mesh was applied. The very strict difficulty appeared when the large plastic deformation of the face of the body approached nodal points too closely. In such a case the only solution was to coarsen the mesh or to reduce the time step. The mesh adaptive technique seems to be appropriate.

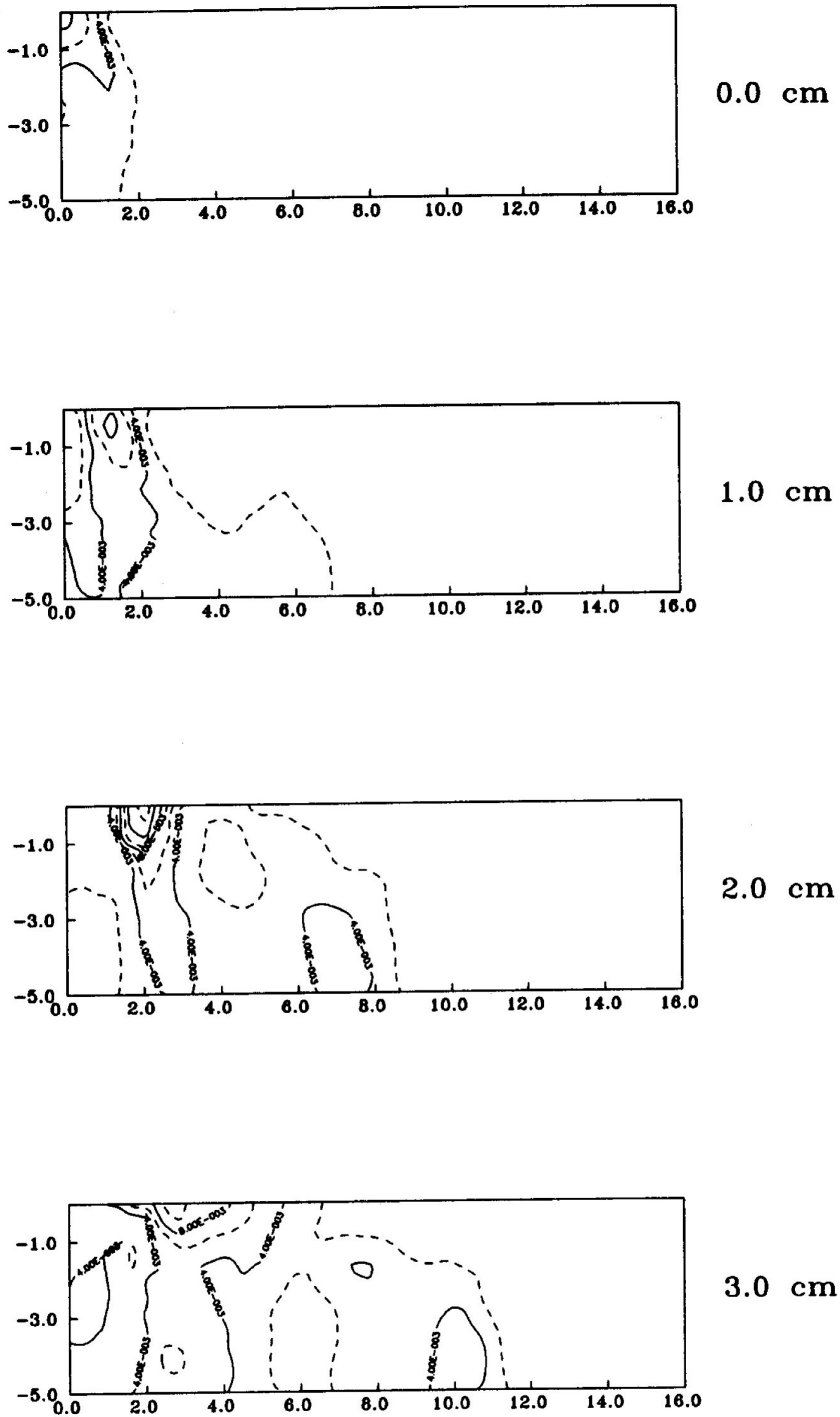


Fig. 7. Second invariant of stresses in successive stages.

In addition, the evolution of the collision process was investigated based on the constant and adaptive mesh discretization. Comparison of displacements in time for the constant meshes and the adaptive one shows the improvement in results when the adaptive technique is applied (Fig. 13).

6. CONCLUSIONS

The application of the adaptive technique to the solution of dynamic contact problems was presented. The use of the space-time element method is expensive since a great number of coefficients has to be determined in one computational step. Here we gain

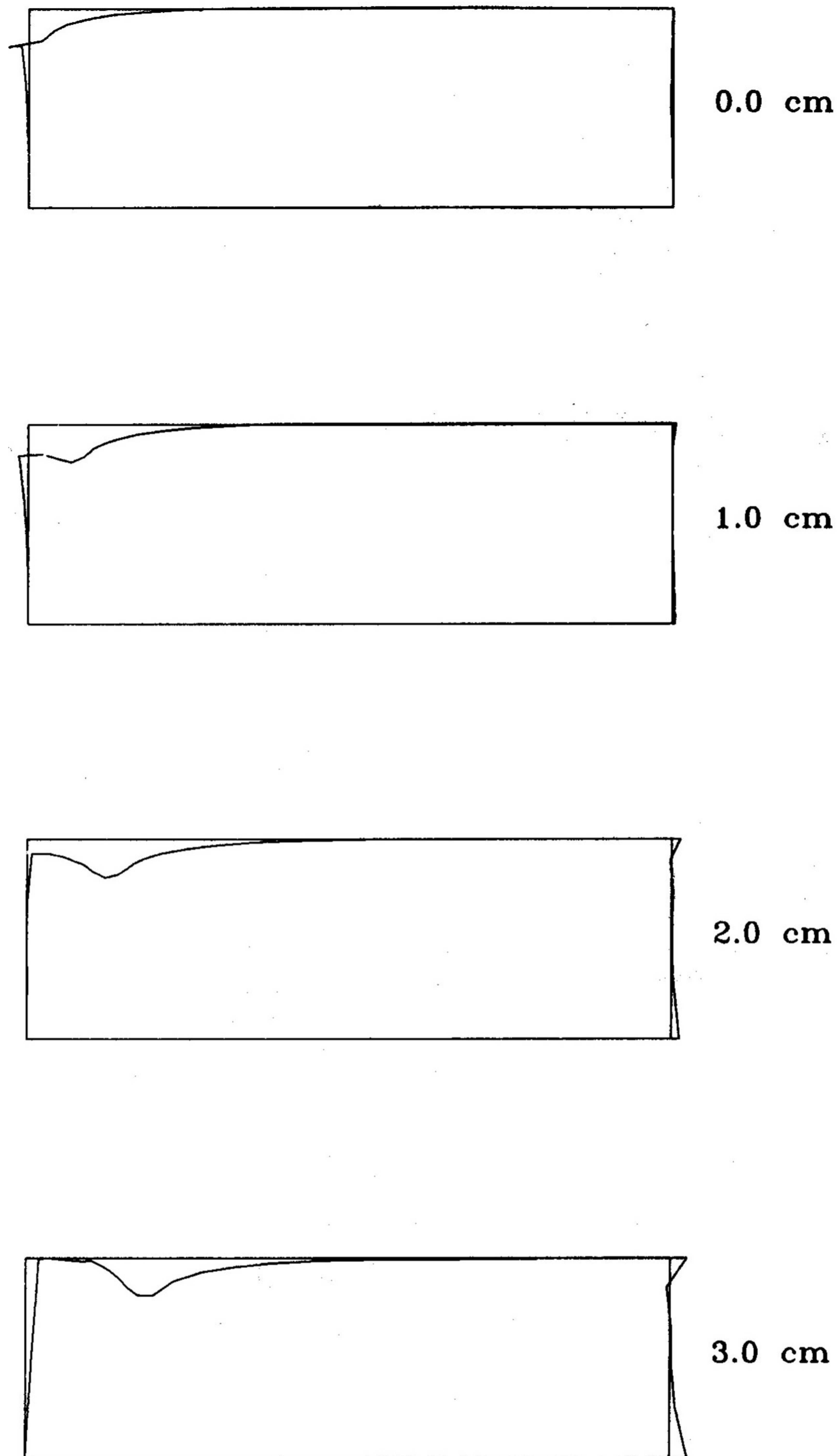


Fig. 8. Deformations (magnified by 50) in successive stages.

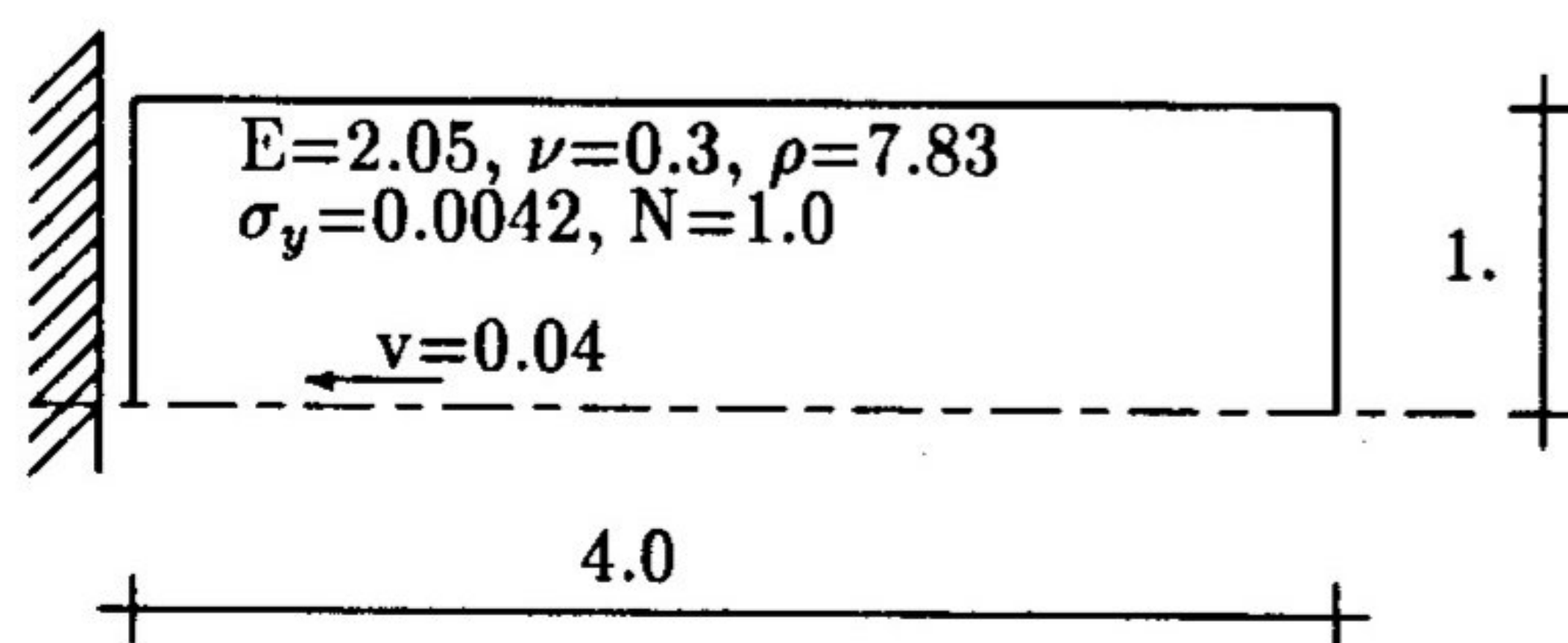


Fig. 9. Collision of the bar—example.

the possibility of simple mesh modification in time. Since the coarse mesh can be applied the total numerical cost decreases in the resulting algorithm. The total cost is a linear function of the number of joints for the arbitrary dimensionality of the structure and this feature may be attractive. In the case of large plastic deformations we can protect the mesh against distortion or approaching of joints. Several testing

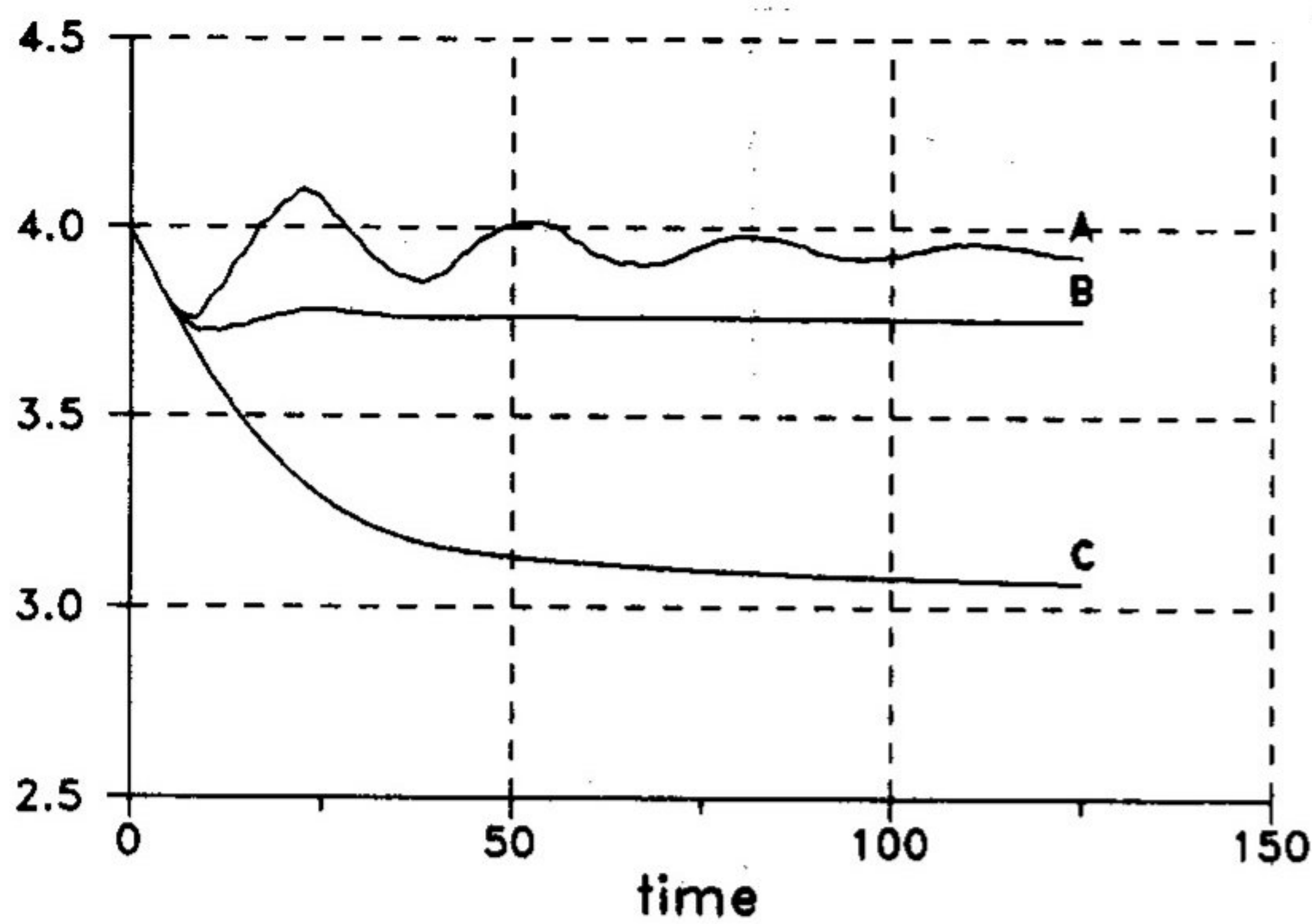


Fig. 10. Comparison of horizontal displacements of the free end in time for: (A) $\gamma = 5 \times 10^{-5}$; (B) $\gamma = 5 \times 10^{-4}$; and (C) $\gamma = 5 \times 10^{-3}$.

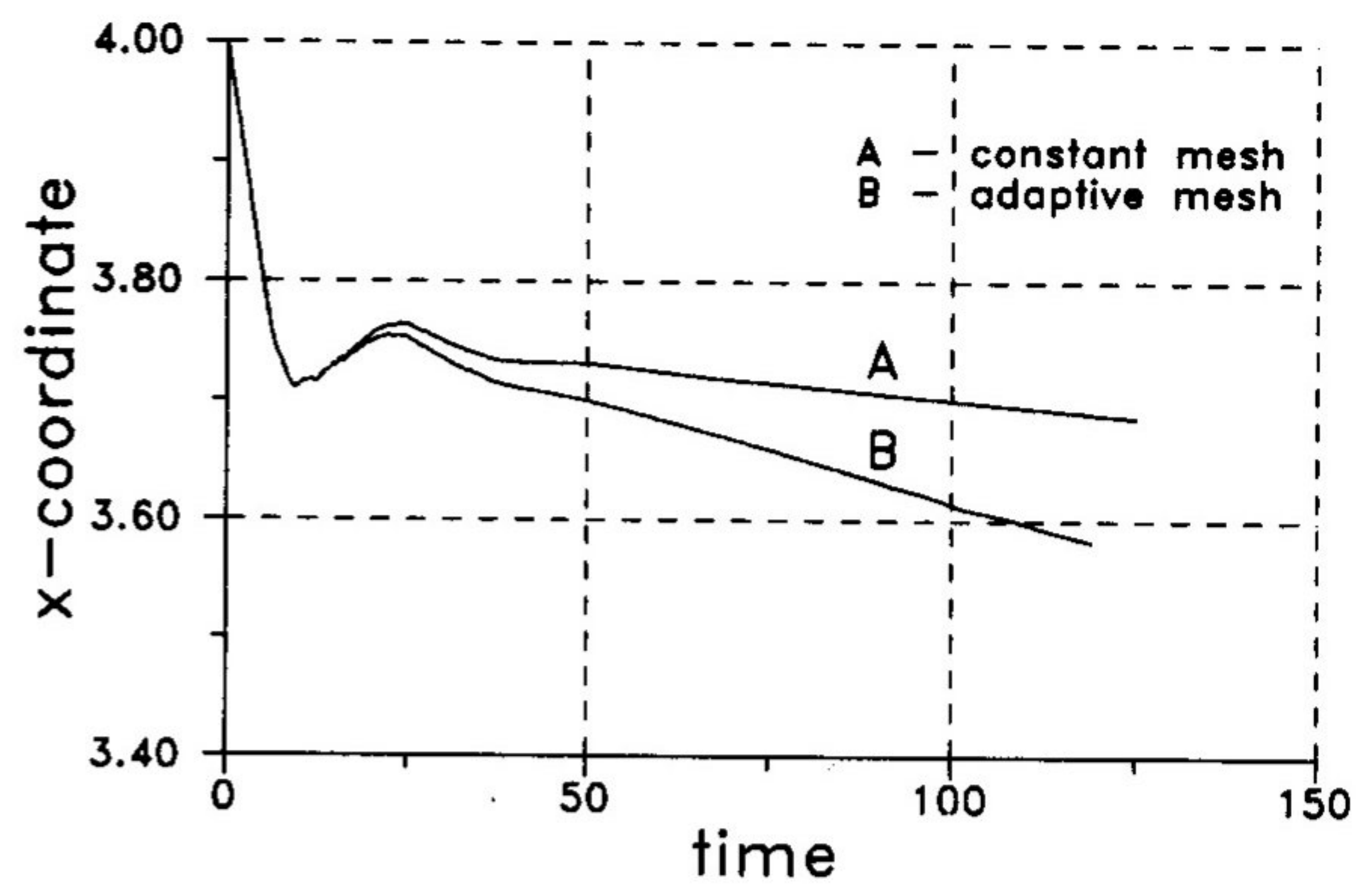


Fig. 13. Displacements in time of the free end for constant and adapted mesh.

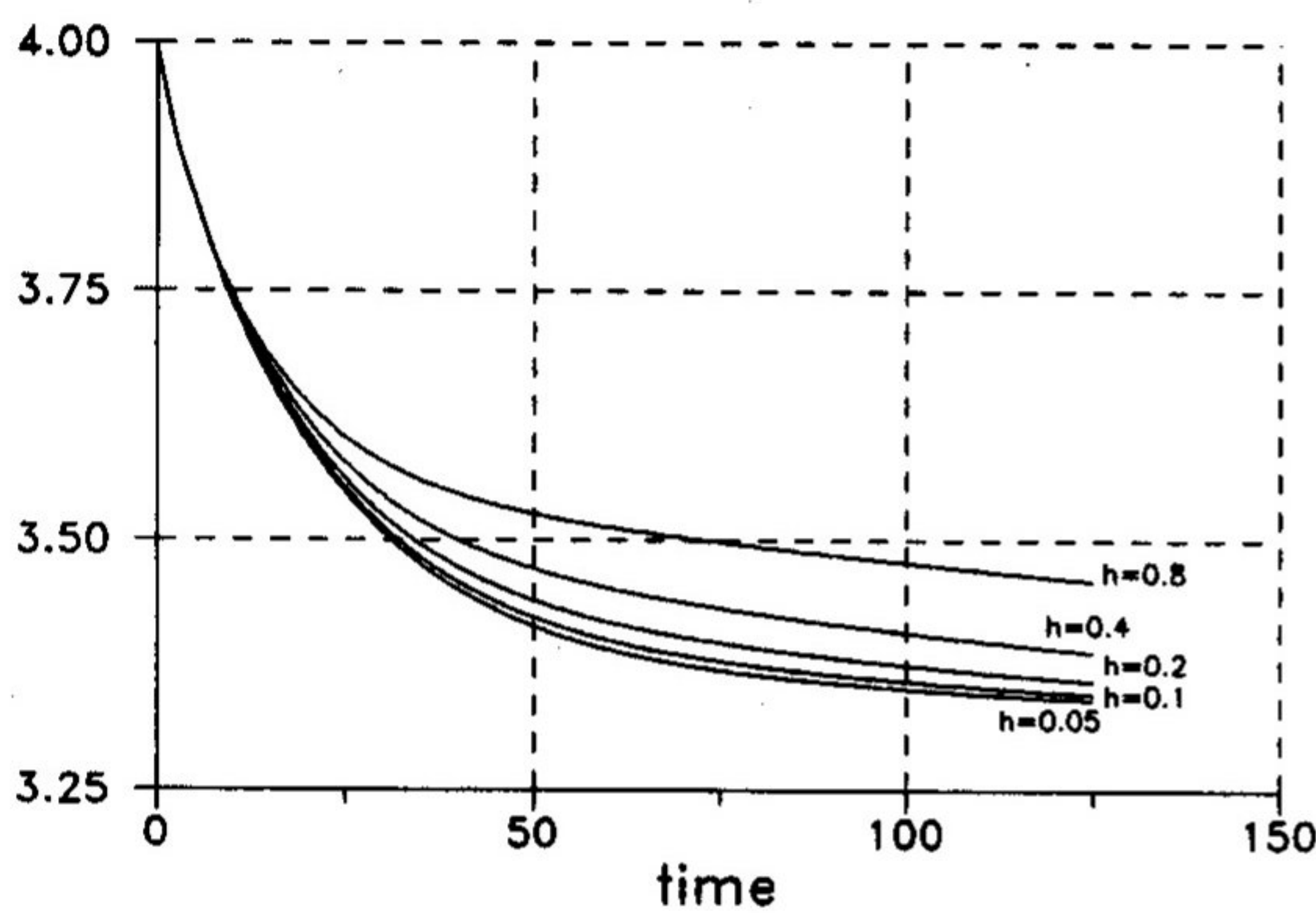


Fig. 11. Comparison of horizontal displacements of the free end in time for different time steps.

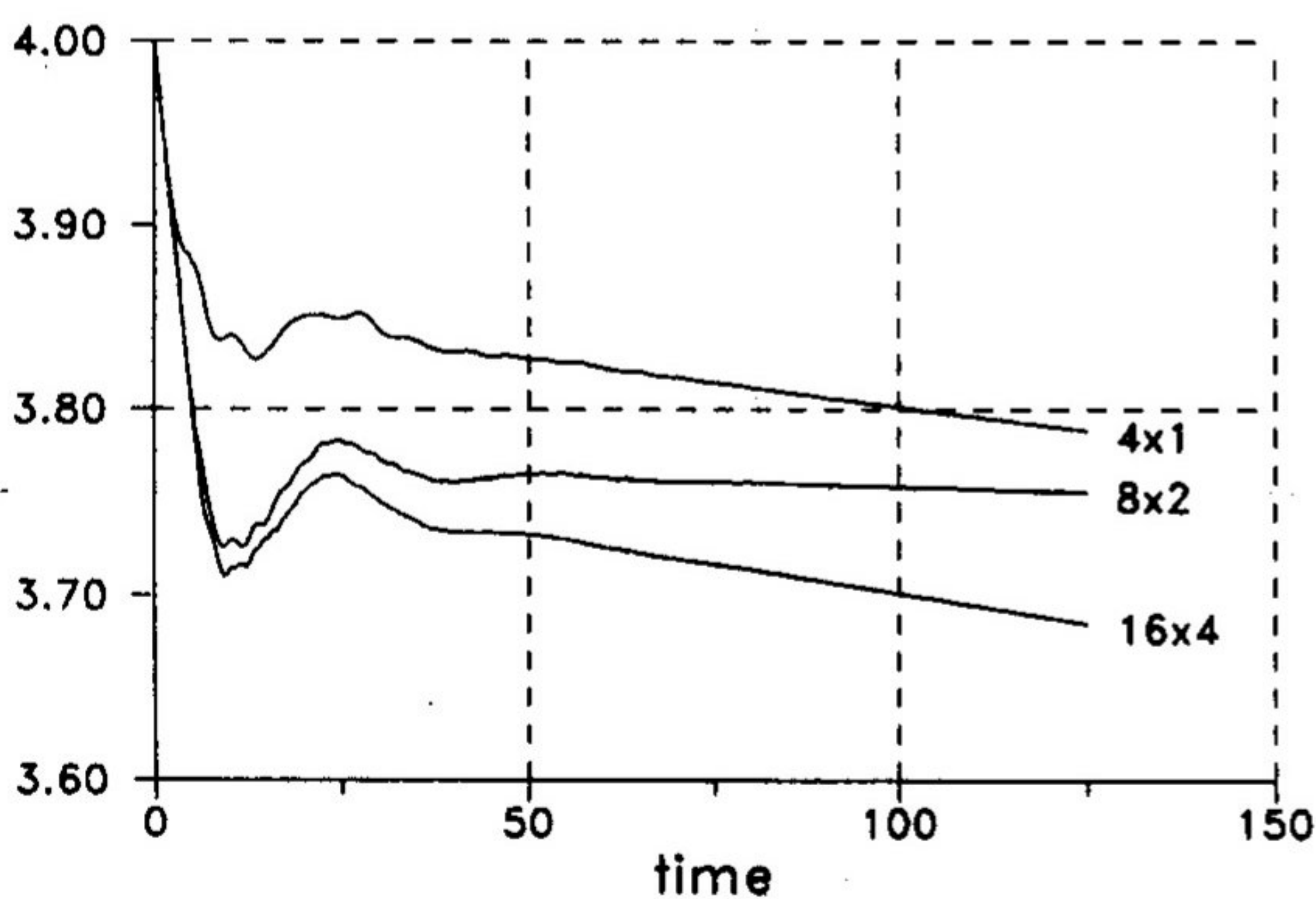


Fig. 12. Comparison of horizontal displacements of the free end in time for selected mesh densities.

solutions prove the efficiency of the presented approach in selected problems.

The appropriate error estimator is still a separate problem. Applied formulas should provide the minimum error not in a single step, as it is in elliptic problems, but in a considered time interval that contains a great number of steps. Experience on this subject is limited.

REFERENCES

1. M. J. Baines and A. J. Wathen, Moving finite element methods for evolutionary problems. I. Theory. *J. Comput. Phys.* **79**, 245-269 (1988).
2. I. W. Johnson, A. J. Wathen and M. J. Baines, Moving finite element methods for evolutionary problems. II. Applications. *J. Comput. Phys.* **79**, 270-297 (1988).
3. C. I. Bajer, Triangular and tetrahedral space-time finite elements in vibration analysis. *Int. J. Numer. Meth. Engng* **23**, 2031-2048 (1986).
4. C. I. Bajer and C. G. Bonthoux, State-of-the-art in true space time finite element method. *Shock Vibr. Dig.* **20**, 3-11 (1988).
5. C. I. Bajer, Adaptive mesh in dynamic problem by the space-time approach. *Comput. Struct.* **33**, 319-325 (1989).
6. C. I. Bajer, Notes on the stability of non-rectangular space-time finite elements. *Int. J. Numer. Meth. Engng* **24**, 1721-1739 (1987).
7. T. J. R. Hughes and G. M. Hulbert, Space-time element methods for elastodynamics: formulations and error estimates. *Comput. Meth. appl. Mech. Engng* **66**, 339-363 (1988).
8. G. M. Hulbert, Space-time finite element method for second-order hyperbolic equation. Ph.D. thesis, Stanford University, CA (1989).
9. K. J. Bathe, *Finite Element Procedures in Engineering Analysis*. Prentice-Hall, Englewood Cliffs, NJ (1982).
10. W. Olszak and P. Perzyna, Stationary and non-stationary visco-plasticity form. In *Inelastic Behaviour of Solids* (Edited by M. F. Kanninen, W. F. Adler and A. R. Rosenfeld). McGraw-Hill, New York (1970).
11. P. Perzyna, Fundamental problems in viscoplasticity. *Advances Appl. Mech.* **9**, 243-377 (1966).
12. O. C. Zienkiewicz and O. Corneau, Visco-plasticity by the finite element process. *Arch. Mech.* **24**, 873-888 (1972).
13. O. C. Zienkiewicz and J. Z. Zhu, A simple error estimator and adaptive procedure for practical engineering analysis. *Int. J. Numer. Meth. Engng* **24**, 337-357 (1987).
14. J. Zhu and O. C. Zienkiewicz, Adaptive techniques in the finite element method. *Commun. appl. Numer. Meth.* **4**, 197-204 (1988).
15. O. C. Zienkiewicz, J. Z. Zhu and N. G. Gong, Effective and practical h - p -version adaptive analysis procedures for the finite element method. *Int. J. Numer. Meth. Engng* **28**, 879-891 (1989).
16. D. J. Benson, An efficient, accurate, simple ALE method for nonlinear finite element programs. *Comput. Meth. appl. Mech. Engng* **72**, 305-350 (1989).